International Journal of Engineering & Technology, 4 (2) (2015) 311-319
www.sciencepubco.com/index.php/IJET
©Science Publishing Corporation
doi: 10.14419/ijet.v4i2.4432
Research Paper

Validation of leak test models for pharmaceutical isolators

Shih-Cheng Hu [1], Angus Shiue [1]*, Yu-Min Hsu [1], Yi-Sung Ke [2]

[1] *Department of Energy and Refrigerating Air-conditioning Engineering, National Taipei University of Technology, Taipei, TAIWAN*
[2] *Yun Lin Technology Co. Ltd*
**Corresponding author E-mail: angusshiue@gmail.com*

Copyright © 2015 Angus Shiue et al. This is an open access article distributed under the Creative Commons Attribution License, which permits unrestricted use, distribution, and reproduction in any medium, provided the original work is properly cited.

Abstract

In this study, we performed three leak tests on a side-recirculated air isolator: a particle-count test, performed at a variety of positive and negative pressures; the SF_6 trace gas method, performed at a variety of airflow velocities; and a pressure decay method, performed at a variety of initial pressures. From the particle-count test, we measured particle leak ratios of 30–34% for pressures of −18 to −25 Pa. In contrast, using the SF_6 tracer gas method. we measured leak ratios of 7.8%, 5.9%, and 3.8% for airflow velocities of 0.61, 0.51, and 0.41 m/s, respectively. The particle-count test detected leaks quickly and easily, but its leak ratio was overly high because it included particles from outside of the chamber as well as from the filter. Although the SF_6 tracer gas method took more time, it was more sensitive and accurate. The leak quantity would be affected by air velocity and the pressure. Leak concentration acted as sterilization phase of isolator that would result in concentration distributed nonhomogeneous phenomena; concentration distributed from outside of the chamber can be acted as a leakage diffusion situation of contaminants leak. Using the pressure decay method to compare downward airflow through a raised-floor and side-wall return air isolators, the fall time, leak quantity, and leak area of the downward airflow through a raised-floor isolator was five times greater, four times les, and 4.5 times less than that of the side-wall return-air isolator, respectively. According to idea gas law, keeping the temperature and pressure of the chamber constant will effectively reduce the leak quantity.

Keywords: *Isolator; Leak Test; Particle Count Method; SF6 Tracer Gas Method; Pressure Decay Test.*

1. Introduction

Isolators have been used by the pharmaceutical industry since the early 1980s and by the nuclear industry since the 1950s. Isolators make an airtight barrier or enclosure around a lump of equipment or process to separate it from the operator, who can execute tasks through half-suits or glove ports. Isolators supply a controlled environment by applying HEPA filters to supply an ISO class five airflow, which is then typically recirculated by returning it to air handlers through sealed ductwork. Many environment variables in an isolator can be controlled, including its pressure (positive or negative), humidity, oxygen, and airflow directionality. Using an isolator protects the product from the operator (by maintaining aseptic conditions) and protects the operator from the product (by isolating the hazard).
Today, isolator technology is described in all major directives (Food and Drug Administration (FDA), U.S. Pharmacopeial Convention (USP), The Pharmaceutical Inspection Convention and Pharmaceutical Inspection Co-operation Scheme (PIC/S), ph. Eur., International Organization for Standardization (ISO), Virtual Desktop Infrastructure (VDI), etc.) and supported by the large pharmaceutical communities (International Society of Pharmacoepidemiology (ISPE), the Pharmacists' Defence Association (PDA), Arbeitsgemeinschaft for Pharmazeutische Verfahrenstechnik (APV)) [1-10]. Isolators must be tested for leaks periodically to ensure process safety, containment of hazardous materials or products dangerous to personnel or environment, and operator safety during bio-decontamination [11]. The accepted isolator specific leak rate, defined in ISO 14644-7:2004 [6] and ISO 10648-2:1994 [12], is based on acceptable operational exposure limits (OEL) for particular applications. The number and size of chamber penetrations must be minimized to reduce leaking and fulfill the ISO requirement. Leak testing can be performed using different methodologies, containing pressure decay or chemical detection. Nevertheless, measurement

processes of the leak-rate and the detection of leak place are very different. The leak-rate is explained as the quantity of air leaked per unit of time from a positive or negative space. Common presentation of leak-rate is the percentage loss of volume per hour [11], [13]. In comparison, leak detection is performed to find the location of the leak after an isolator fails a leak-rate test.

The main target of this study is to determine leak reduction of the downward airflow through a raised-floor and side-wall return air isolator by using a particle-count test, the SF_6 tracer gas method, and a pressure decay test. It also investigates how the face velocity of the fan and sampling position affect the leak rate of the isolator.

2. Methods and materials

2.1. Equipment setup

It is a closed loop composed by inlet fans and inlet filters in charge of the generation of the unidirectional air flow inside the isolator. At the bottom of each isolator section, all the air is extracted by the fans in charge of the recirculation, and re-introduced in the isolator chamber via the filtration stage. We used the side-wall and downward airflow through raised-floor return-air methods to detect leaks in the isolator. Both, air is supplied from an inflow HEPA filters in the supply air plenum and this flows vertically through the isolator, and recirculated inward airflow from direct side-wall and indirect side-wall with down return-air way through downflow HEPA filters, respectively. For the side-wall return air isolator, we used either particles or a tracer gas to detect the location of the leak (see Figure (1)). We then used a pressure decay test to quantitatively analyze the leak measurements for both the side-wall air isolator and the downward airflow through a raised-floor isolator (see Figure (2)). The main chamber volume, outlet area, and return area of the side-wall return-air isolator are 1 × 0.74 × 0.7 m, 0.72 × 0.35 m, and 0.79 × 0.49 m, respectively, while those dimensions of the downward airflow through a raised-floor return-air isolator are 1.2 × 1 × 0.82 m, 1.2 × 0.6 m, and 0.82 × 0.82 × 0.6 m, respectively.

2.2. Particle count method

In general, pharmaceutical cleanrooms and associated controlled environments are classified based on ISO 14644-1[14]. In the standard, the cleanliness level is so-called ISO class N, which indicates the maximum allowable particle number concentrations for particle sizes ranging from 0.1 µm up to 5.0 µm in form of the equation:

$$C_n = 10^N \times (\frac{0.1}{D})^{2.08} \quad (1)$$

Where C_n is the maximum number concentration of airborne particles (particle number/m^3 of air), which are equal to or larger than the specific particle size. The number N is the ISO class number, which is less or equal to 9. D is the specific particle size in µm.

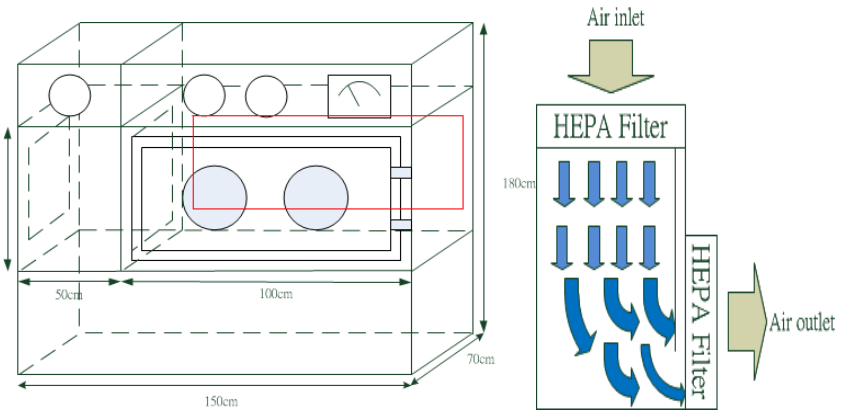

Fig. 1: Schematic of a Side-Wall Air Isolator. The Red Box Indicates the Return Location.

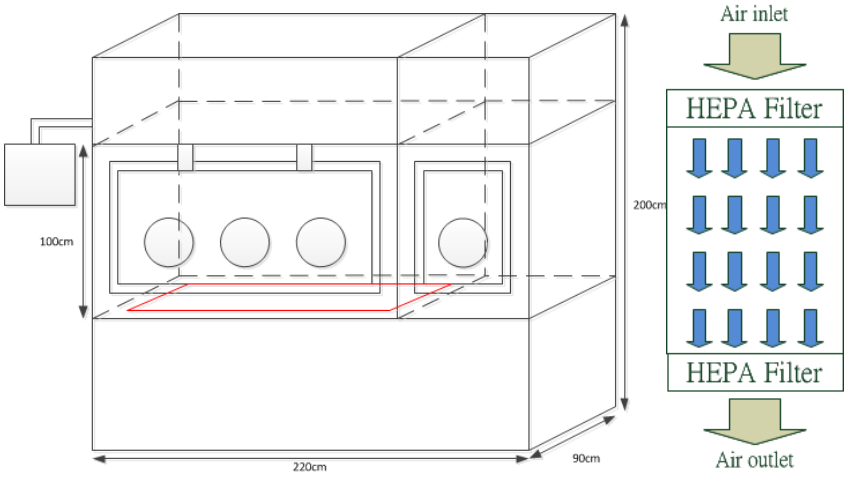

Fig. 2: Schematic of the Downward Airflow through a Raised-Floor Isolator. The Red Box Indicates the Return Location.

Apart from the concentration of the particles scene, the profile of particles should be drawn, donating the particle size distribution. A multi-point laser particle counter (Pacific Scientific Model Met One 2100.10, Ashtead Technology) was used to record particle concentrations every 30 s at four different locations in the main chamber of the side-wall return-air isolator. (See Figure (3)) these measurements were taken at positive pressures of 18, 20, and 22 Pa (changed by adjusting the fan speed) and negative pressures of −18, −20, and −22 Pa (changed by adjusting a vacuum pump) in the main chamber of the isolator.

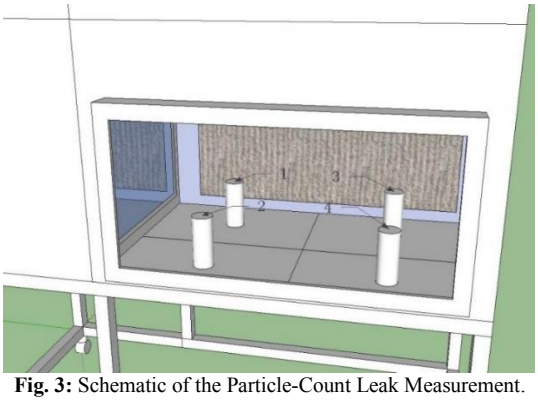

Fig. 3: Schematic of the Particle-Count Leak Measurement.

2.3. SF_6 tracer gas method

Keeping the side-wall isolator at positive pressure and normal operating conditions, we placed a sensor outside of the chamber to monitor the decay of SF_6 concentration every 150 s for 25 minimums at three fan speeds. We injected a maximum SF_6 concentration of 550 ppm. We monitored the following areas of the isolator: 1) inside the chamber, 2) outside of the chamber, 3) between the glove and sub-chamber, 4) between the supply air layer and outside of the chamber, and 5) between sensing points 1 and 2 in the chamber (see Figure (4a)), and sensing points 2), 3), and 4) outside the chamber, as shown in Figure (4b-4d).

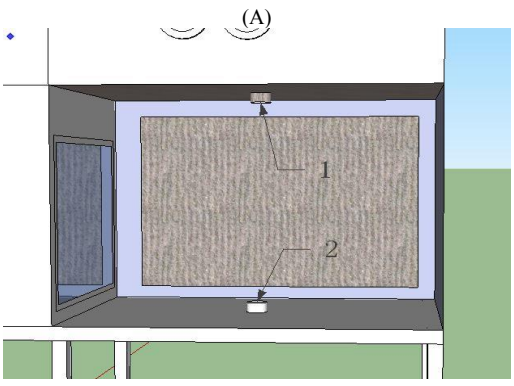

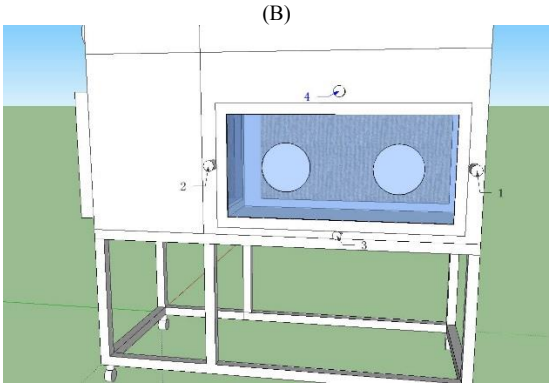

(C) (D)

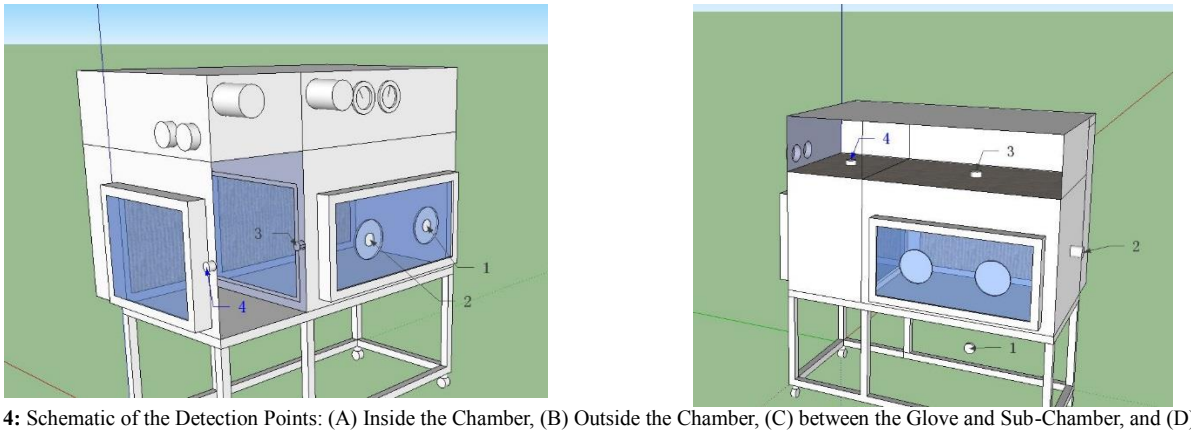

Fig. 4: Schematic of the Detection Points: (A) Inside the Chamber, (B) Outside the Chamber, (C) between the Glove and Sub-Chamber, and (D) at the Supply-Air Plenum.

Provided that no tracer gas is supplied to the isolator during the measurement and the airflow through the isolator is constant, the concentration of tracer gas decays exponentially with time. By drawing the natural logarithm of gas concentration against time, we obtain a straight line; the gradient of it is the air-exchange rate (A) on the isolator [15]:

$$C = C_0 \exp(-A \bullet t) \tag{2}$$

Where C_0 is the concentration at time t = 0.

Equation (1) is often re-arranged in the following form:

$$\ln C = \ln C_0 - A \bullet t \tag{3}$$

2.4. Pressure decay test

This experiment is a static test that compares the side-wall airflow (not fully welded) and downward airflow through raised-floor (fully welded) isolators. First, we shut off the power and the sealed the return airport and air outlet, and then injected dry air into the chamber to bring the pressure inside the chamber to four times greater than the normal pressure. After these steps, we observed the pressure differential by using a pressure meter, and recorded the time required for the pressure to drop to the initial pressure. The volumetric leak rate was determined as follows [6], [12], [16]:
For an isolator whose volume is V (m^3):

$$Volume\ loss\ per\ \text{second} = \frac{V \times n}{3600} m^3 s^{-1} \tag{4}$$

$$n = \frac{P_1 - P_2}{P_2} \frac{3600}{\text{decay time}} (h^{-1}) \tag{5}$$

Where P_1 is the starting pressure (Pa), and P_2 is the end pressure (Pa).

3. Results and discussion

3.1. Particle counte method

Figure (5) shows particle concentration profiles in an isolator at various positive pressures (18, 20, and 22 Pa) and negative pressures (−18, −25, and −30 Pa) for various particle sizes. Table 1 shows logarithmic empirical equations of relationships between particle concentration and diameter. In all these tests, the concentration of leaking particles progressively increases as the absolute value of the pressure increases, whether negative or positive. For the side-wall return-air isolator, the percentage of leaking particle is 30–34% from −18 to −25 Pa.

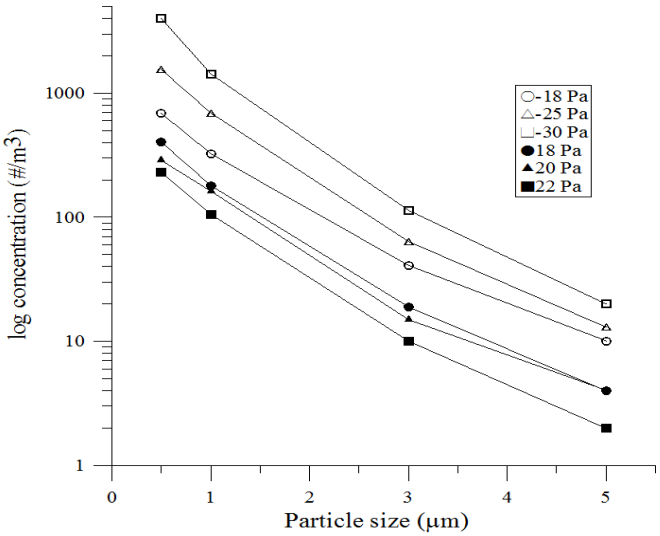

Fig. 5: Profiles of Particle Concentrations at Various Positive and Negative Pressures.

Table 1: Correlations of Particle Concentration with Particle Size

Pressure (Pa)	Particle concentration vs. particle size
−18	C_n = −297.2 ln D+452.72, R^2=0.9867
−25	C_n = −669.3 ln D+1006.4, R^2=0.9836
−30	C_n = −1761 ln D+2613.8, R^2=0.9831
18	C_n= −179 ln D+269.92, R^2=0.9871
20	C_n = −127.1 ln D+191.51, R^2=0.9861
22	C_n = −98.7 ln D+148.72, R^2=0.982

3.2. SF_6 tracer gas method

2

3.2.1. Inside the chamber

Figure (6) shows the concentration profiles of SF_6 over time inside the chamber at different airflow velocities (0.41, 0.51, and 0.61 m/sec) and positions. Table 2 shows logarithmic empirical equations of relationships between SF_6 concentration and testing time. In all these tests, the SF_6 leak concentration increases with the airflow velocity; the SF_6 leak percentages are 3.7, 5.9, and 7.8% at airflow velocities of 0.41, 0.51, and 0.61 m/sec, respectively.

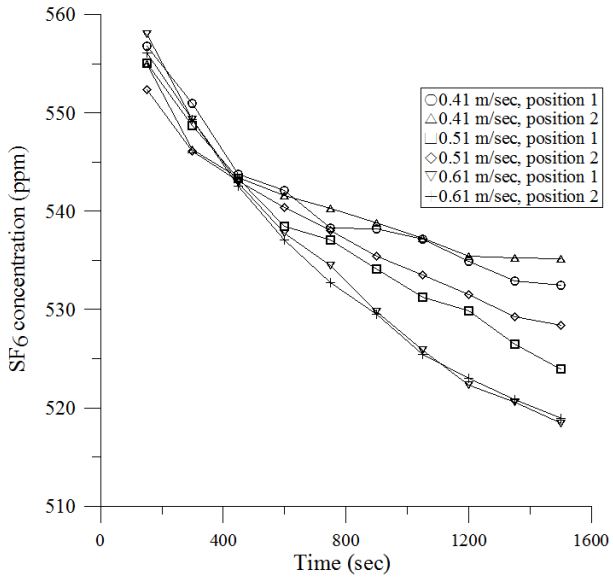

Fig. 6: Profiles of SF_6 Concentrations at Different Positions with Different Airflow Velocities, Measured Inside the Chamber.

Table 2: Correlations of SF_6 Concentration with Testing Time inside the Chamber

Air velocity (m/s)	Position	SF_6 concentration vs. testing time
0.41	1	C= −10.72 ln t+610.68, R^2 = 0.9868
	2	C = −8.386 ln t+595.55, R^2 = 0.9806
0.51	1	C = −13.3 ln t+623.8, R^2 = 0.981
	2	C = −10.4 ln t+606.2 R^2 = 0.983
0.61	1	C = −17.7 ln t+649.6, R^2 = 0.983
	2	C = −17.0 ln t+644.4, R^2 = 0.982

3.2.2. Outside the chamber

The outside doors of the isolator often open and close without exposing the main chamber, as shown in Figure (4b); this experiment inspected the gas-seal tightness between the outside and the main chamber. Figure (7) shows SF_6 concentration profiles over time outside the chamber at various airflow velocities (0.41, 0.51, and 0.61 m/sec) and positions. Table 3 shows logarithmic empirical equations of relationships between the SF_6 concentration and testing time.

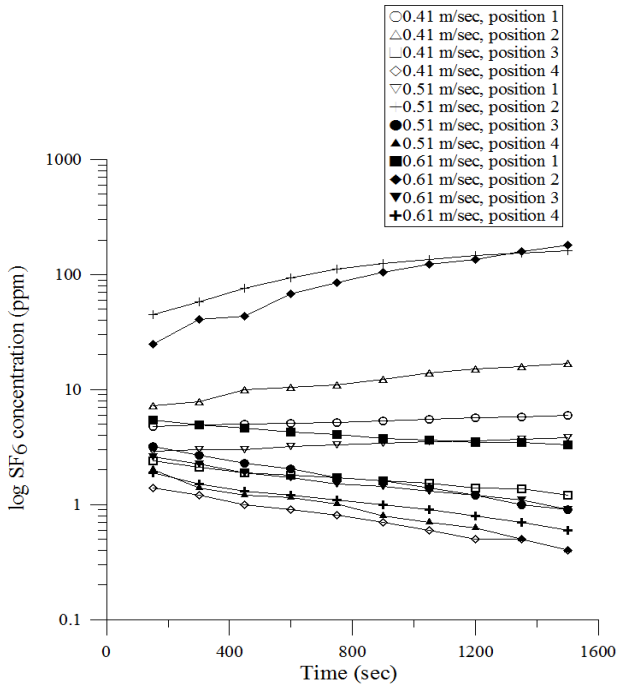

Fig. 7: Profiles of SF_6 Concentration at Different Positions with Different Airflow Velocities, Measured Outside the Chamber.

3.2.3. Gloves and sub-chamber

Isolator gloves are often used incorrectly or improperly stretched, and the pressure of the sub-chamber is usually lower than that of the main chamber, as shown in Figure (4c). Figure (8) shows the SF_6 concentration profiles over time outside the chamber at various airflow velocities (0.41, 0.51, and 0.61 m/sec) and positions. Table 4 shows logarithmic empirical equations of relationships between the SF_6 concentration and testing time.

Table 3: Correlations of SF_6 Concentration with Testing Time outside the Chamber

Air velocity (m/s)	Position	SF_6 concentration (y) vs. testing time (x)
0.41	1	C= 0.513 ln t+1.937, R^2 = 0.981
	2	C= 4.219ln t−15.35, R^2 = 0.986
	3	C= −0.492 ln t+4.9, R^2 = 0.981
	4	C= −0.442 ln t+3.68, R^2 = 0.983
0.51	1	C = 0.425 ln t+0.54, R^2 = 0.982
	2	C = 55.644 ln t−252.49, R^2 = 0.981
	3	C= −1.02 ln t+8.455, R^2 = 0.986
	4	C= −0.653ln t+5.238, R^2 = 0.982
0.61	1	C= −0.952 ln t+10.3, R^2 = 0.983
	2	C = 58.33 ln t−282.34, R^2 = 0.983
	3	C= −0.72 ln t+6.31, R^2 = 0.988
	4	C = −0.534 ln t+4.58, R^2 = 0.988

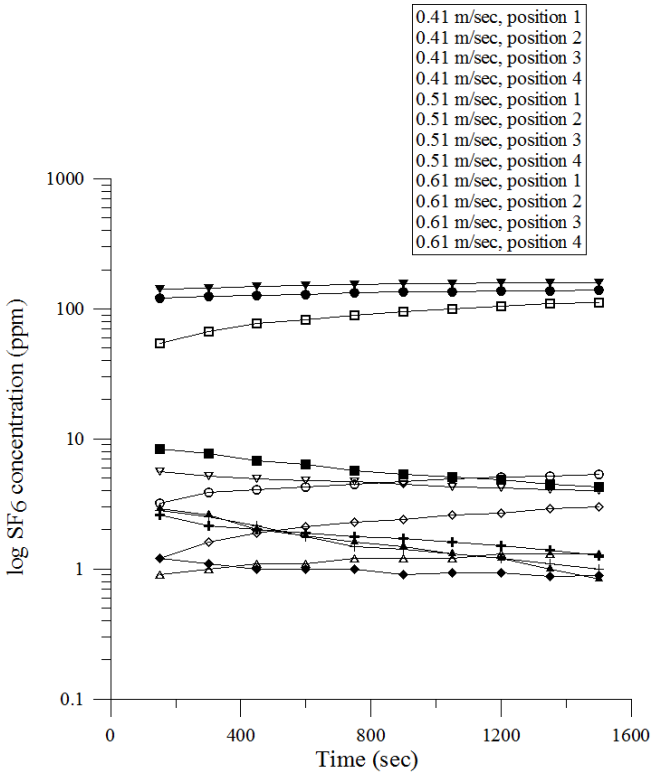

Fig. 8: Profiles of SF_6 Concentrations at Different Positions with Different Airflow Velocities, Measured at the Glove and Sub-Chamber.

Table 4: Correlations of SF_6 Concentration with Testing Time, Measured at the Glove and Sub-Chamber

Air velocity (m/s)	Position	SF_6 concentration (y) vs. testing time (x)
0.41	1	C= 0.895 ln t−1.32, R^2 = 0.985
	2	C= 0.181 ln t−0.02, R^2 = 0.965
	3	C= 25.906 ln t−79.58, R^2 = 0.985
	4	C= 0.78 ln t−2.821, R^2 = 0.981
0.51	1	C= −0.697 ln t+9.18, R^2 = 0.982
	2	C= −0.833 ln t+7.1, R^2 = 0.982
	3	C= 8.473 ln t+76.64, R^2 = 0.984
	4	C= −0.911 ln t+7.616, R^2 = 0.982
0.61	1	C= −1.872 ln t+18.102, R^2 = 0.983
	2	C= −0.139 ln t+1.889, R^2 = 0.946
	3	C= 8.462 ln x+97.71, R^2 = 0.981
	4	C= −0.534 ln t+5.27, R^2 = 0.984

3.2.4. Supply-air plenum

The supply-air plenum of the main chamber and sub-chamber are isolated from each other, as shown in Figure (4d). Considering the internal air recirculation, the released SF_6 concentration at position 5 and inside the chamber are normally the same. However, the supply-air plenum of the sub-chamber did not generate SF_6 and may leak through into the environment. Figure (9) shows SF_6 concentration profiles over time outside the chamber at various airflow velocities (0.41, 0.51, and 0.61 m/sec) and positions. Table 5 shows logarithmic empirical equations of relationships between the SF6 concentration and testing time.

3.3. Pressure decay method

The initial pressure inside the chamber inside was based on a flow meter reading of 100 LPM. After filling the chamber to a critical pressure, we then let the pressure inside the chamber decay naturally to five Pa and recorded the fall time. We repeated the experiment by increasing the flow in increments of 10 LPM up to 180 LPM. The fall time of natural decay of the downward airflow through a raised-floor isolator was four times greater than that of the side-wall return air isolator, as shown in Table 6. Figure (10) shows quadratic empirical equations of relationships between the fall time and leak rate; the leak areas of the side-wall return-air and downward airflow through a raised-floor isolator are 0.0689–0.0886 m^2 and 0.0137–0.018 m^2, respectively.

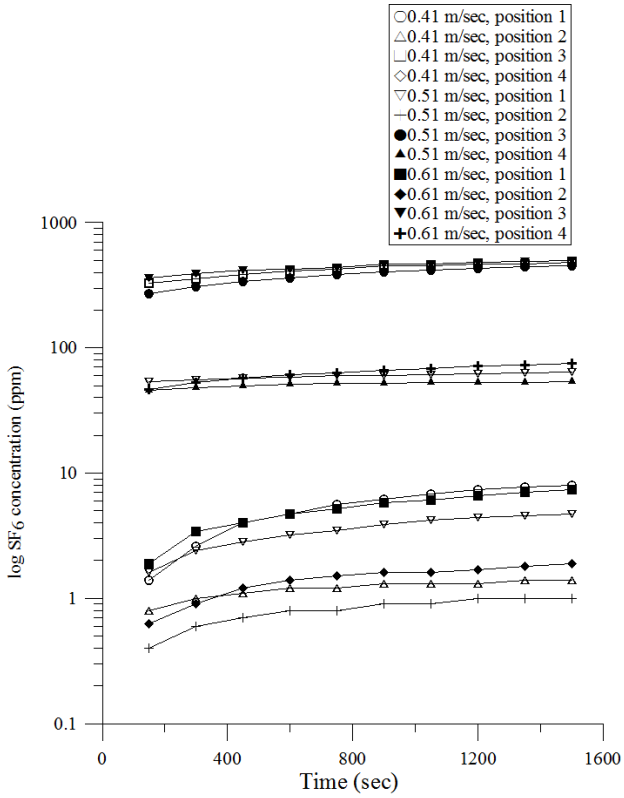

Fig. 9: Profiles of SF_6 Concentrations at Different Positions for Different Airflow Velocities through the Supply-Air Plenum.

4. Conclusion

In the present study, we investigated leakage reduction in the downward airflow through a raised-floor and side-wall return air isolators by using particle-count tests, the SF_6 tracer gas method, and a pressure decay test. We also investigated how the face velocity of the fan and the sampling position affect the leak rate of the isolator. For the side-wall isolator, the particle leak ratio was 30–34% from −18 to −25 Pa, and the SF_6 leak ratios were 3.7, 5.9, and 7.8% at airflow velocities of 0.41, 0.51, and 0.61 m/sec, respectively. The particle-count method was quick and simple, but measured overly large leak values because it included particles outside the chamber along with those accumulated from the filter and air recirculation. The SF_6 tracer gas method took more time but was more sensitive and accurate. In these experiments, the airflow velocity and pressure affected the measured leak rate. The leak concentration inside and outside the isolator is heterogeneous phenomena of the concentration profile while sterilization period and leak diffusion of the contaminant, respectively. The fall time of the natural decay of the fully welded isolator was four times greater than that of the partially welded isolator. The leak area of the partially welded isolator was 4.5 times greater than that of the fully welded isolator. Based on the ideal gas law, keeping a constant temperature and pressure inside the chamber will effectively decrease the leak rate.

Table 5: Correlations of SF_6 Concentration with Testing Time, Measured at the Supply- Air Plenum.

Air velocity (m/s)	Position	SF_6 concentration (y) vs. testing time (x)
0.41	3	C= 3.024 ln t−14.28, R^2 = 0.984
	4	C= 0.255 ln t−0.46, R^2 = 0.983
	5	C= 69.063 ln t−27.82, R^2 = 0.982
	6	C= 4.413 ln t+30.85, R^2 = 0.982
0.51	3	C= 1.392 ln t−5.55, R^2 = 0.986
	4	C= 0.267 ln t−0.93, R^2 = 0.986
	5	C= 82.206 ln t−154.37, R^2 = 0.987
	6	C = 3.329 ln t+29.43, R^2 = 0.985
0.61	3	C= 2.337 ln t−10.04, R^2 = 0.985
	4	C= 0.548 ln t−2.15, R^2 = 0.989
	5	C= 60.034 ln t+51.60, R^2 = 0.986
	6	C = 12.311 ln t−16.98, R^2 = 0.984

Table 6: Leak Test Data Taken Using the Pressure Decay Method.

Initial pressure (Pa)	Final pressure (Pa)	Side-wall return air isolator			Downward airflow through a raised-floor isolator		
		Fall time (s)	Leak rate (m^3/s)	Leak area (cm^2)	Fall time (s)	Leak rate (m^3/s)	Leak area (cm^2)
136	5	20	$5.022\times.0^{-5}$	0.0882	152	7.807×10^{-6}	0.0137
165	5	22	5.576×10^{-5}	0.0886	162	8.947×10^{-6}	0.0142
191	5	26	5.500×10^{-5}	0.0811	181	9.334×10^{-6}	0.0138
236	5	34	5.209×10^{-5}	0.0689	190	1.101×10^{-5}	0.0146
264	5	34	5.841×10^{-5}	0.0730	194	1.209×10^{-5}	0.0151
300	5	35	6.463×10^{-5}	0.0756	198	1.349×10^{-5}	0.0158
333	5	35	7.186×10^{-5}	0.0798	200	1.485×10^{-5}	0.0165
367	5	39	7.117×10^{-5}	0.0752	205	1.599×10^{-5}	0.0169
435	5	40	8.243×10^{-5}	0.0799	210	1.855×10^{-5}	0.0180

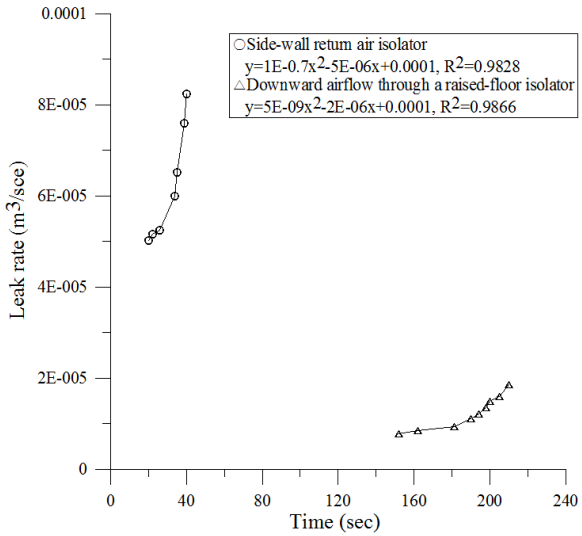

Fig. 10: Relationship between Fall Time and Leak Rate.

Acknowledgements

The authors would like to acknowledge the supports from Yun Lin Technology Co., LTD. in Taiwan.

References

[1] Food and Drug Administration, Guidance for Industry, "Sterile Drug Products Produced by Aseptic Processing," September (2004), www.fda.gov.
[2] United States Pharmacopeia, "Sterility Testing – Validation of Isolator Systems," USP XXIII Informational Chapter 1208, Pharmacopeial Forum 23 No. 6, (1997).
[3] United States Pharmacopeia 27 and National Formulary 22, "Pharmaceutical Compounding – Sterile Preparations," Chapter 797, 319 - 336.
[4] PIC/S Recommendation "Isolators Used for Aseptic Processing and Sterility Testing," presented at the *Pharmaceutical Inspection Convention*, June (2002).
[5] European Commision, Directive 2003/94/EC, annex 1, "Manufacture of sterile Medicinal Products," May (2003), Revision (2008).
[6] International Standard, ISO 14644-7, "Cleanrooms and Associated Controlled Environments" Part 7 Separative Devices (Clean Air Hoods, Gloveboxes, Isolators and Mini Environments) (2004).
[7] International Society for Pharmaceutical Engineering, ISPE, *Annual Barrier Isolation Conference*, www.ispe.org.
[8] Parenteral Drug Association, PDA, Technical Report No. 34 "Design and Validation of Isolator Systems for the Manufacturing and Testing of Health Care Products," September/October (2001), www.pda.org.
[9] Arbeitsgemeinschaft fur Pharmazeutische Verfahrenstechnik APV, "From Cleanroom to Isolator Technology," APV Course, Basel/Switzerland, May (2008).
[10] Verein Deutscher Ingenieure VDI, VDI 2083, Blatt 16, Barrieresysteme, under work; http://www.vdi.de.
[11] Arvind Asthana, A., "Isolator: Case study of Issues Involved", Pharma Times Vol. 43, No. 10 (2011) 31.
[12] ISO 10648-2:1994, "Containment enclosures -- Part 2: Classification according to leak tightness and associated checking methods".
[13] Coles, T., "Leak rate measurement for pharmaceutical isolators: Practical guidance for operators and test engineers", Clean Air and Containment Review, Vol. 11 (2012) 8-12 (2012).
[14] International Standard, ISO 14644-1, "Cleanrooms and Associated Controlled Environments" Part 1 Classification of air cleanliness, (1999).
[15] Lagus, P.L., "Control Room In leakage Measurements using Tracer Gas Techniques", Vent (2006). http://dx.doi.org/10.3320/1.2759030.
[16] Midcalf, B., W. M. Phillips, J. S. Neiger, and T. J. Coles, "Pharmaceutical Isolators. Pharmaceutical Press", (2004).